IEEE/CSC & ESAS EUROPEAN SUPERCONDUCTIVITY NEWS FORUM (ESNF), No. 10, October 2009.
Published in *AIP Conference Proceedings* **1218**, pp. 1581-1592 (2010)

Optimiation Calculations for a 30 HZ, 4 K Regenerator with Helium-3 Working Fluid*

Ray Radebaugh[1], Yonghua Huang[2], Agnes O'Gallagher[1], and John Gary[1]

[1]National Institute of Standards and Technology
Boulder, Colorado, 80305, USA

[2]Shanghai Jiao Tong University
Shanghai, China

ABSTRACT

The NIST numerical software, REGEN3.3, which incorporates both He-4 and He-3 properties, was used to calculate the losses and second law efficiencies of 4 K regenerators operating at 30 Hz. Operating parameters, such as average pressure, pressure ratio, and warm-end temperature were varied to investigate the effect of non-ideal gas properties. Regenerator parameters such as matrix material and shape, hydraulic diameter, and regenerator geometry were varied to investigate losses due to non-ideal regenerator behavior. The results show that He-3 can increase the regenerator efficiency by a factor of at least two compared to a regenerator optimized for He-4. A layered regenerator of gadolinium oxysulfate (GOS) at the cold end and ErPr at the warm end is the best of many material combinations. A regenerator with parallel holes of about 20 % porosity showed only slight improvement over one with packed spheres. The regenerator warm-end temperature has little effect on its efficiency for temperatures below 35 K and pressures of 1.0 MPa and above. An optimized 4 K He-3 regenerator uses layered GOS and ErPr with the warm end at about 30 K and an average pressure of about 1.0 MPa. With those optimum conditions a reduced regenerator loss of 0.36 and a regenerator second law efficiency of 25 % are achieved.

KEYWORDS: Cryocoolers, cryogenics, efficiency, Gifford-McMahon, helium-3, helium-4, numerical analysis, pulse tubes, real gas, refrigeration, regenerators, Stirling, theory

INTRODUCTION

The application of low temperature superconducting (LTS) systems, such as magnetic resonance imaging (MRI) systems utilizing superconducting magnets or electronic devices

utilizing Josephson junctions, requires the use of 4 K cryocoolers. Typically these cryocoolers have been either Gifford-McMahon (GM) cryocoolers or GM-type pulse tube cryocoolers that operate at frequencies of about 1 Hz [1]. The efficiencies of these cryocoolers are in the range of 0.5 to 1.0 % of Carnot, whereas 80 K cryocoolers often achieve efficiencies of at least 15 % of Carnot. The low efficiencies of 4 K cryocoolers leads to large compressors with large input powers. The low operating frequency of the GM and GM-type pulse tube also leads to large temperature oscillations at the cold end at the operating frequency of the cryocooler. The amplitude of the temperature oscillation decreases as the cryocooler operating frequency is increased. Higher frequencies also allow the use of Stirling cryocoolers or Stirling-type pulse tube cryocoolers, which have much higher efficiencies in converting electrical power to PV power in the pressure oscillator. These frequencies are typically in the range of 30 to 60 Hz. However, these higher frequencies generally lead to greater losses in the regenerator unless careful optimization is carried out. Recent work with a 4 K GM-type pulse tube [2, 3] and a Stirling-type pulse tube cryocooler [4] has shown that the use of ^{3}He instead of ^{4}He increased the cooling power for the same power input. Previous modeling efforts by us [5, 6] have shown that the loss associated with real gas effects in the regenerator can be significantly reduced by using ^{3}He at a relatively low average pressure of 0.5 to 1.0 MPa instead of ^{4}He at the normal pressure of 1.5 to 2.5 MPa. A layered regenerator matrix of gadolinium oxysulfate (GOS) at the cold end and $Er_{0.5}Pr_{0.5}$ at the warm end was found to minimize the losses in a 4 K regenerator with the warm end at 20 K [6]. In this paper we model the effects of many parameters on the performance of 4 K regenerators to arrive at an optimized set of parameters that maximizes the regenerator efficiency.

NUMERICAL MODEL

Helium-3 properties

The Debye equation used to express the temperature dependence of the specific heat of solids was used by Huang *et al.* [7, 8] to fit published experimental data for the thermodynamic properties of ^{3}He for temperatures from 0.01 K to 1500 K and pressures up to 20 MPa. Deviations between this Debye equation of state and the reference experimental data were within ±1 %. Because there are no experimental data for the transport properties of ^{3}He in the gas phase, a quantum version of the principle of corresponding states was used to calculate the viscosity, thermal conductivity, and surface tension of ^{3}He in the gas phase [5]. The equations for both the thermodynamic and transport properties of ^{3}He were incorporated into the numerical model discussed below.

NIST Numerical Model REGEN3.3

The results presented in this paper were obtained with the new version 3.3 of the NIST numerical regenerator model REGEN3.3 that includes an option to select ^{4}He or ^{3}He as the working fluid as well as the ideal gas version of either gas. The boundary conditions for the older versions, 3.1 or 3.2 [9] required the mass flow to be given at both ends of the regenerator. In the new version the mass flow and pressure at the cold end are inputs. This avoids an iteration to guess the mass flow at the warm end to obtain the pressure ratio and phase relative to the cold end mass flow. The latter usually determine the desired operating point for the model. Other changes and comparisons with the older version were discussed previously [5]. The excellent convergence of the new version at 4 K made the calculations

for this work straightforward. Running times with a desktop computer were typically about 20 minutes for a 4 K regenerator.

CRYOCOOLER THERMODYNAMICS

Regenerative Cryocooler Losses

Only the last-stage regenerator, which reaches 4 K, is considered in the analysis presented here. The time-averaged acoustic power $\langle P\dot{V}\rangle_h$ that drives this stage enters the regenerator at the hot end at a temperature of T_h. It is defined by the reversible isothermal power input given by the time-averaged Gibbs free energy flow $\langle \dot{G}\rangle_h$. The purpose of the regenerator is to deliver to the cold end as much of this acoustic power as possible with a minimum of losses. For Stirling or Gifford-McMahon cryocoolers the displacer at the cold end produces a time-averaged expansion power $\langle \dot{W}\rangle_{\exp}$ that leads to a net refrigeration power given by

$$\dot{Q}_{net} = \langle \dot{W}\rangle_{\exp} - \langle \dot{H}\rangle_{reg} - \dot{Q}_{cond} - \dot{Q}_{rad}, \tag{1}$$

where $\langle \dot{H}\rangle_{reg}$ is the time-averaged enthalpy flow in the regenerator, with positive numbers referring to flow from the warm end to the cold end, $\dot{Q}_{cond}$ is the conduction heat leak through the regenerator, and $\dot{Q}_{rad}$ is the radiative heat leak to the cold end, which is ignored in this work. The expansion power is related to the isothermal reversible power or acoustic power at the cold end $\langle P\dot{V}\rangle_c$ by

$$\langle \dot{W}\rangle_{\exp} = \langle \dot{W}\rangle_{rev} - \dot{Q}_{pt} = \langle P\dot{V}\rangle_c - \dot{Q}_{pt}, \tag{2}$$

where $\dot{Q}_{pt}$ is the loss associated with an imperfect pulse tube or any irreversible expansion process at the cold end. The introduction of acoustic power in equation (2) makes it valid for pulse tube cryocoolers as well as for Stirling and Gifford-McMahon cryocoolers.

The loss associated with the enthalpy flow $\langle \dot{H}\rangle_{reg}$ in the regenerator can be divided into two parts, as given by

$$\langle \dot{H}\rangle_{reg} = \langle \dot{H}\rangle_P + \dot{Q}_{reg}, \tag{3}$$

where $\langle \dot{H}\rangle_P$ is the enthalpy flow associated with the enthalpy pressure dependence (real gas effect) and $\dot{Q}_{reg}$ is the thermal loss associated with enthalpy flow caused by imperfect heat transfer and limited heat capacity in the regenerator (regenerator ineffectiveness). This separation allows us to determine the intrinsic loss associated with use of a real gas and how that differs between ^{4}He and ^{3}He. Both gas properties and regenerator properties affect $\dot{Q}_{reg}$. Combining equations (1), (2), and (3) gives us

$$\dot{Q}_{net} = \langle P\dot{V}\rangle_c - \langle \dot{H}\rangle_P - \dot{Q}_{reg} - \dot{Q}_{cond} - \dot{Q}_{pt}. \tag{4}$$

We can define the gross refrigeration power as that associated with a perfect regenerator and a perfect expansion process, which then gives [5]

$$\dot{Q}_{gross} = \langle P\dot{V}\rangle_c - \langle \dot{H}\rangle_P = \langle P\dot{V}\rangle_c \left[1 - \frac{\langle \dot{H}\rangle_P}{\langle P\dot{V}\rangle_c}\right]. \quad (5)$$

Equations (4) and (5) can be combined to give

$$\dot{Q}_{net} = \langle P\dot{V}\rangle_c \left[1 - \frac{\langle \dot{H}\rangle_P}{\langle P\dot{V}\rangle_c}\right]\left[1 - \frac{\dot{Q}_{reg}}{\dot{Q}_{gross}} - \frac{\dot{Q}_{cond}}{\dot{Q}_{gross}} - \frac{\dot{Q}_{pt}}{\dot{Q}_{gross}}\right]. \quad (6)$$

The acoustic power anywhere along the regenerator with perfect heat transfer and no pressure drop varies as the specific volume. In the presence of a pressure drop, the cold-end acoustic power is related to the hot-end acoustic power by

$$\langle P\dot{V}\rangle_c = \left(Z_c T_c / Z_h T_h\right)\left(\langle P\dot{V}\rangle_h - \langle \Delta P\dot{V}\rangle_h\right), \quad (7)$$

where Z_c is the compressibility factor at the cold end, Z_h is the compressibility factor at the hot end, and $\langle \Delta P\dot{V}\rangle_h$ is the additional acoustic power required at the hot end due to pressure drop in the regenerator. By substituting equation (7) into equation (6) we can express the net refrigeration power as

$$\dot{Q}_{net} = \langle P\dot{V}\rangle_h \left[1 - \frac{\langle \Delta P\dot{V}\rangle_h}{\langle P\dot{V}\rangle_h}\right]\left[\frac{Z_c T_c}{Z_h T_h}\right]\left[1 - \frac{\langle \dot{H}\rangle_P}{\langle P\dot{V}\rangle_c}\right]\left[1 - \frac{\dot{Q}_{reg}}{\dot{Q}_{gross}} - \frac{\dot{Q}_{cond}}{\dot{Q}_{gross}} - \frac{\dot{Q}_{pt}}{\dot{Q}_{gross}}\right]. \quad (8)$$

By writing the net refrigeration power in this manner, we have separated out the terms that are functions only of the gas properties from those that also depend on the hardware. The first factor on the right hand side of the equation is the acoustic power input at the hot end of the regenerator. The second factor shows the effect of pressure drop in the regenerator and is both hardware and gas dependent. The third factor shows the reduction in acoustic power due to temperature change and real-gas behavior associated with compressibility. The fourth factor shows the effect of real-gas enthalpy flow. The terms in the last set of brackets are both hardware and gas dependent.

FIGURE 1 shows a schematic of the energy flows and losses associated with the last stage of a regenerative cryocooler as represented by equation (8). The relative magnitudes shown for each of the acoustic power flows and the losses are typical of a regenerative cryocooler at 4 K. As this figure shows, the losses are quite large, and the remaining net refrigeration power is quite small compared to the input power.

Coefficient of performance and efficiency

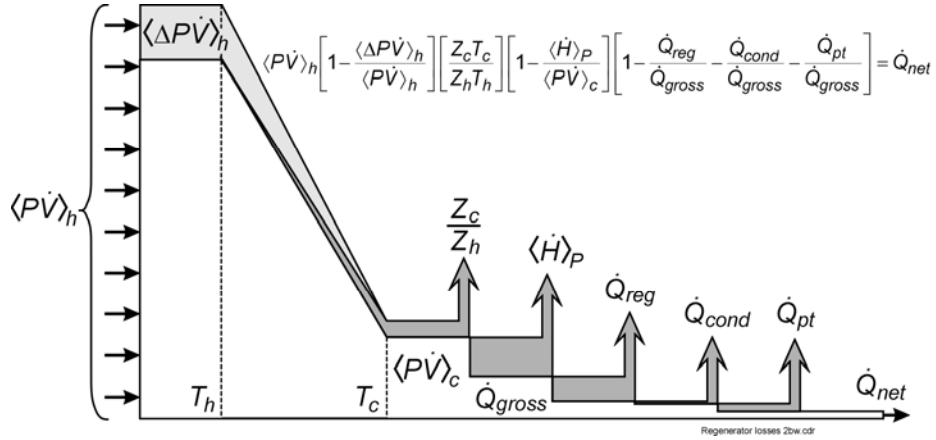

FIGURE 1. Diagram showing energy flows and losses in a regenerator and pulse tube.

The coefficient of performance of the last stage regenerator is given by

$$\mathrm{COP} = \frac{\dot{Q}_{net}}{\langle P\dot{V}\rangle_h}. \tag{9}$$

For an ideal gas and a perfect regenerator, the ideal COP for this last-stage regenerator is given by (T_c/T_h), where we assume that the reversible expansion work at the cold end is not being fed back to the hot end of this regenerator. Thus, the thermodynamic second-law efficiency of the last stage is given by

$$\eta = (T_h/T_c)\mathrm{COP}. \tag{10}$$

Combining equations (8), (9), and (10) gives the second law efficiency of the last stage as

$$\eta = \left[1 - \frac{\langle \Delta P\dot{V}\rangle_h}{\langle P\dot{V}\rangle_h}\right]\left[\frac{Z_c}{Z_h}\right]\left[1 - \frac{\langle \dot{H}\rangle_P}{\langle P\dot{V}\rangle_c}\right]\left[1 - \frac{\dot{Q}_{reg}}{\dot{Q}_{gross}} - \frac{\dot{Q}_{cond}}{\dot{Q}_{gross}} - \frac{\dot{Q}_{pt}}{\dot{Q}_{gross}}\right]. \tag{11}$$

Equation (11) also expresses the ratio of the net entropy input at the cold end $\dot{Q}_{net}/T_c$ to the time-averaged entropy flow at the warm end of the regenerator $\langle \dot{S}\rangle_h$. In the work presented here we assume the pulse tube loss is zero, so the efficiency values are those of only the regenerator.

REAL GAS EFFECTS

When only the real gas effects are taken into account, the net refrigeration power equals the gross refrigeration power, as given by equation (5). For a perfect regenerator the lost acoustic power due to pressure drop in equation (7) is zero. The efficiency for a perfect last stage becomes

$$\eta_{gross} = \frac{Z_c}{Z_h}\left(1 - \frac{\langle \dot{H}\rangle_P}{\langle P\dot{V}\rangle_c}\right). \tag{12}$$

The enthalpy flow associated with the real gas effects can be found by using a first law energy balance on the regenerator with perfect isothermal heat exchangers on each end along with the condition that the hot-blow stream must be warmer than the cold-blow stream. Details of this calculation have been discussed previously [5]. FIGURE 2

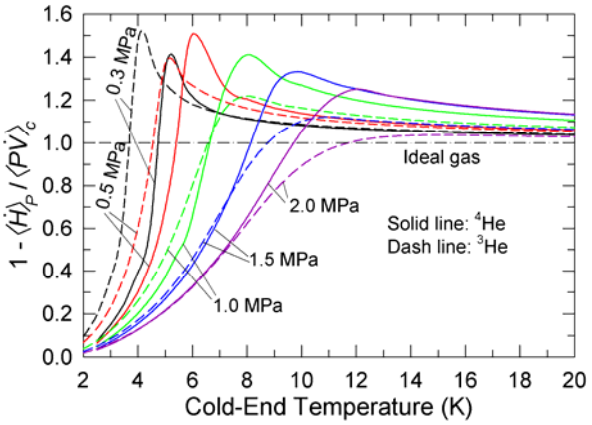

FIGURE 2. Ratio of real gas COP to ideal gas COP for last stage of a perfect regenerative cryocooler.

compares the efficiency given by equation (12) for ^{4}He and ^{3}He working fluids. This figure shows that for temperatures below about 7 K ^{3}He gives a much higher gross efficiency than that given by ^{4}He. This figure also shows that for ^{3}He a reduction of the average pressure to about 0.5 MPa significantly increases the efficiency, whereas the lower pressure actually decreases the efficiency slightly at 4 K for ^{4}He.

PARAMETERS AFFECTING REGENERATOR PERFORMANCE

TABLE 1 lists the many parameters that can affect regenerator performance. The real-gas effects are influenced by the working fluid and by the operating conditions. Losses associated with a non-perfect regenerator are affected by the matrix material, geometry, and operating conditions. In TABLE 1, V_{rg} is the volume of gas in the regenerator, V_E is the swept volume of gas at the regenerator cold end, L is the regenerator length, D_h is the hydraulic diameter of the matrix, n_g is the porosity, P_0 is the average pressure, P_r is the pressure ratio, f is the frequency, T_h is the hot-end temperature, and ϕ_c is the phase by which the mass flow at the cold end leads the pressure at the cold end. In our previous work and in this work, all modeling included both ^{4}He and ^{3}He while varying the other parameters. We have shown previously that the optimum ratio V_{rg}/V_E is in the range of about 7 to 10 for a wide range of pressures, pressure ratios, frequencies, and lengths, but the effect of T_h and regenerator material on this parameter was not investigated [5]. Our previous work focused primarily on a fictitious layered regenerator material called Mix 1 in REGEN3.3 that has the volumetric heat capacity given by a series of several real materials, where the material with the highest volumetric heat capacity at any given temperature is used. The materials in Mix 1 are $Er_{0.9}Yb_{0.1}Ni$ (9 K), $ErAl_2$ (12 K), $ErDy_{0.8}Ni_{0.2}$ (16 K), $Er_{0.6}Pr_{0.5}$ (30 K), and stainless steel, where the temperatures refer to the temperature of the peak heat capacity. REGEN3.3 includes the relatively new regenerator material known as GOS, gadolinium oxysulfate [10], which has a peak at 5.2 K as well as the option to layer any combination of 30 materials in the database while using the maximum volumetric heat capacity or using layers at specified locations. For T_h = 20 K and P_0 = 0.5 MPa we showed that the material combination of GOS + $Er_{0.5}Pr_{0.5}$ gave a lower loss and higher efficiency than any other material combination tested. In this work we examine the effect of material at higher values of T_h and P_0. We also show that the phase angle ϕ_c has a strong effect on the regenerator performance. All the parameters are varied in a way to arrive at an optimum set of conditions for a 4 K regenerator using ^{3}He as the working fluid.

MODELING RESULTS

Optimum Regenerator Volume and Effect of Frequency, Pressure, and Material

FIGURE 3 shows how the reduced regenerator loss varies with reduced regenerator

TABLE 1. Parameters affecting regenerator performance and the range of values studied for each.

Material properties	Working fluid		^{4}He, ^{3}He		
	Regenerator Matrix		9 materials + layers		
Geometry	V_{rg}/V_E	L (mm)	D_h (μm)	Config.	n_g
	3 - 20	10 -50	25 - 60	Spheres, holes	0.1 – 0.7
Operating conditions	P_0 (MPa)	P_r	f (Hz)	T_h (K)	ϕ_c (deg.)
	0.3 -1.5	1.3 - 2	1 - 30	20 - 60	-45 to +30

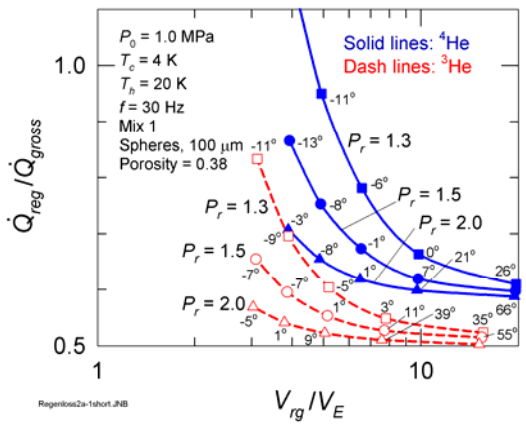

FIGURE 3. Reduced regenerator loss at 30 Hz.

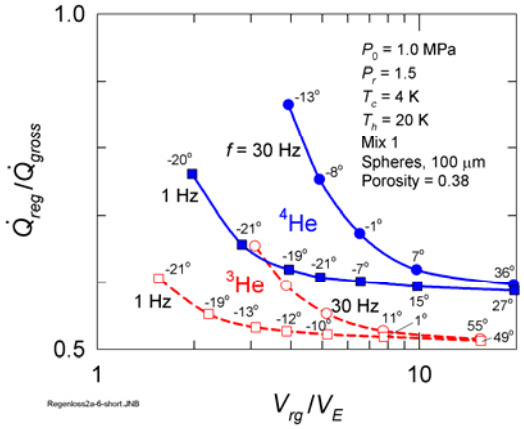

FIGURE 4. Frequency effect on regenerator loss.

gas volume for ^{4}He and ^{3}He for three different pressure ratios at a frequency of 30 Hz. FIGURE 4 shows similar results, but for frequencies of 1 Hz and 30 Hz. For reduced volume ratios between 7 and 10, the higher frequency leads to an increase in the reduced loss for the case of ^{4}He, but frequency has little effect on the loss for ^{3}He. For reduced volume ratios greater than about 10, the phase angle between the flow and pressure at the warm end becomes quite large, which leads to higher losses in the higher temperature regenerators and a large swept volume in the compressor for a given acoustic power. These phase angles are given by the numbers next to each data point in both figures. The maximum allowable reduced regenerator loss would be 1.0 if the compliance tube (pulse tube) had no losses (a figure of merit of 1.0). The pulse tube figure of merit is defined as the ratio of enthalpy flow to acoustic power flow in the pulse tube. When pulse tube losses are taken into account, the net refrigeration power goes to zero when the reduced regenerator loss equals the pulse tube figure of merit. Although this work focuses on losses in the regenerator, typical pulse tube figures of merit are around 0.8, which would be the practical value for the maximum reduced regenerator loss. For 4 K regenerators we found previously that as long as the volume ratio V_{rg}/V_E is in the range of 6 to 10, then area and length have little effect for length for lengths between about 12 mm and 40 mm [6]. All the results discussed here are for a length of 30 mm.

FIGURE 5 shows that the reduced regenerator loss decreases when Mix 1 is replaced with GOS + $Er_{0.5}Pr_{0.5}$ for both 0.5 MPa and 1.0 MPa average pressures, but that the optimum value for V_{rg}/V_E remains in the range of 7 to 10 for ^{4}He but shifts to about 5 to 8 for ^{3}He. The corresponding overall regenerator efficiency (T_h/T_c)COP is shown in FIGURE 6.

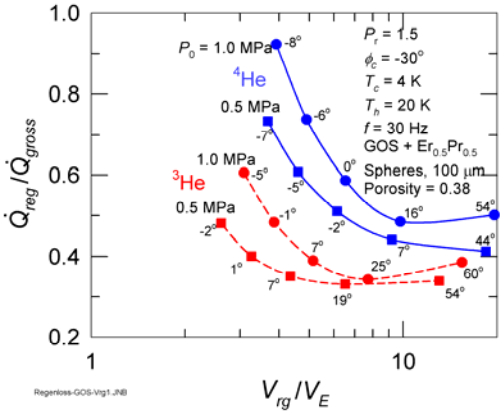

FIGURE 5. Regenerator loss for GOS+$Er_{0.5}Pr_{0.5}$.

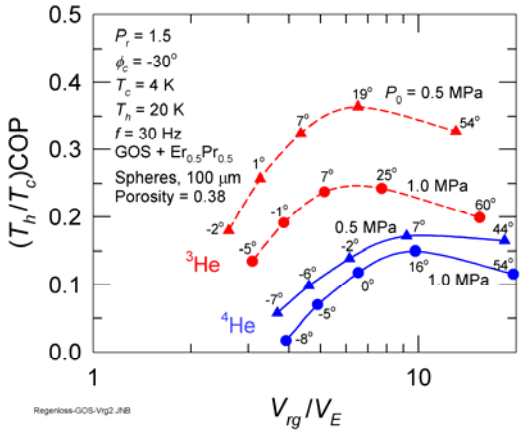

FIGURE 6. Regenerator second law efficiency.

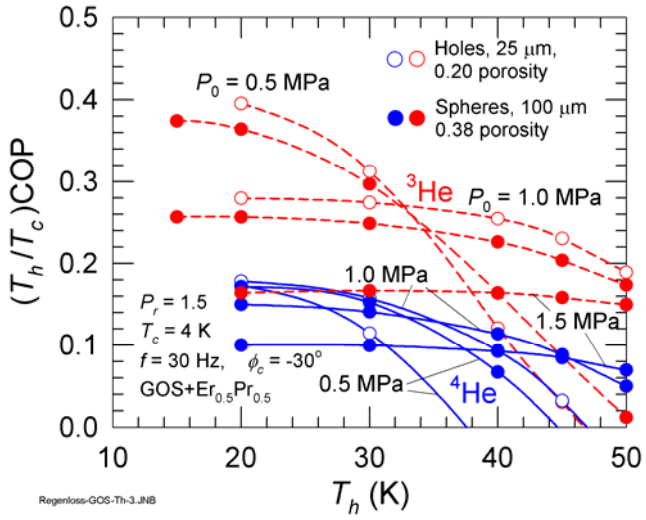

FIGURE 7. Effect of hot temperature and average pressure on regenerator second-law efficiency.

Effect of Hot Temperature and Average Pressure

FIGURE 7 shows the effect of the hot temperature on the efficiency of the regenerator for a matrix of GOS + $Er_{0.5}Pr_{0.5}$ spheres and for the same matrix with 25 μm diameter holes of 20 % porosity. For an average pressure of 1.0 MPa the efficiency decreases very little until the hot temperature exceeds about 35 K. However, for ^{4}He the low efficiency may result in zero net refrigeration when the pulse tube loss is taken into account. The results shown in FIGURE 7 suggest that an optimum hot temperature would be about 30 K to 35 K with an optimum average pressure of 1.0 MPa. Although a higher efficiency can be achieved with P_0 = 0.5 MPa for ^{3}He, a hot temperature of about 25 K or lower is required. The lower pressure would result in reduced efficiencies in the upper regenerator stages and require a pressure oscillator with a larger swept volume. The use of parallel holes increases the efficiency some, as shown in FIGURE 7, but for hot temperatures of 30 K and above the increase is rather small or the efficiency even decreases.

Effect of Matrix Material at T_h = 30 K and P_0 = 1.0 MPa

The layered combination of GOS + $Er_{0.5}Pr_{0.5}$ was found previously to give the highest regenerator efficiency out of eight other combinations of matrix materials, including that of GOS + $HoCu_2$ + $Er_{0.5}Pr_{0.5}$. Those comparisons were for T_h = 20 K and P_0 = 0.5 MPa. FIGURE 8 shows a similar comparison of materials, but for T_h = 30 K and P_0 = 1.0 MPa.

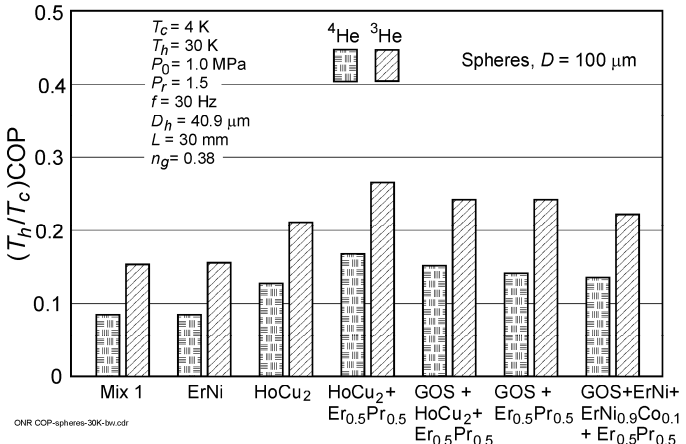

FIGURE 8. Regenerator efficiency for spheres of various materials by use of ^{4}He and ^{3}He.

This comparison shows that at this higher temperature and higher pressure several material combinations yield about the same performance. With these conditions the combination of $HoCu_2$ + $Er_{0.5}Pr_{0.5}$ yields an efficiency very slightly higher than that of GOS + $Er_{0.5}Pr_{0.5}$, but the difference is very small. FIGURE 9 shows the calculated temperature profiles when a matrix of GOS + $Er_{0.5}Pr_{0.5}$ is used. The crossover temperature for the volumetric heat capacity of these two materials is 6.9 K, as shown in FIGURE 10, and the location of this crossover point in the regenerator is shown in FIGURE 9 for both ^{3}He and ^{4}He. The location of this temperature in the regenerator then defines the boundary location between the two materials. FIGURE 10 shows the volumetric heat capacity of the various regenerator materials and that of both ^{4}He and ^{3}He at P_0 = 1.0 MPa.

Effect of Phase Angle ϕ_c, Hot Temperature, and Pressure Ratio

The phase angle between the flow and the pressure affects the flow amplitude, and, therefore, the regenerator loss, for a given acoustic power flow. The minimum loss is expected to occur for flow in phase with the pressure, but that phase can occur at only one location in the regenerator, which should be near the midpoint. For that phase to occur near the midpoint, the phase at the cold end ϕ_c will be approximately -30° (flow lagging pressure). All the results discussed so far are have been for ϕ_c = -30°. Such a phase can be achieved with a Gifford-McMahon (GM) cryocooler or a Stirling cryocooler, where the phase is set by motion of the displacer. In pulse tube cryocoolers the phase at the warm end of the pulse tube needs to be about -60° to achieve ϕ_c = -30°. With a Stirling-type pulse tube cryocooler operating at 30 Hz, a -60° phase at the pulse tube warm end is possible only with a sufficiently large acoustic power flow at the inertance tube entrance [11]. When the warm end of the pulse tube is at a low temperature, such as 30 K, the desired phase can be achieved with less acoustic power. However, for a 4 K pulse tube cryocooler designed for net refrigeration powers less than about 0.5 W, the acoustic power flow is such that the desired -60° phase cannot be achieved, even with the inertance tube at a temperature of 20 K to 30 K. A double inlet can be used along with the inertance tube in such a situation to increase the phase shift, but the additional power flow through the secondary orifice often limits the phase shift to about 30° ($\phi_c \approx 0°$) before the overall cooler efficiency is decreased. Alternatively, a mechanical phase shifter, such as a warm displacer, could be used at the warm end of the pulse tube to achieve any desired phase shift, even in a low-power cryocooler.

FIGURE 11 shows how the regenerator efficiency varies with ϕ_c for hot temperatures of 20 K, 30 K, and 40 K. With a purely resistive impedance $\phi_c \approx +30°$, and according to FIGURE 11, it would not be possible to achieve 4 K with either ^{4}He or ^{3}He when the warm

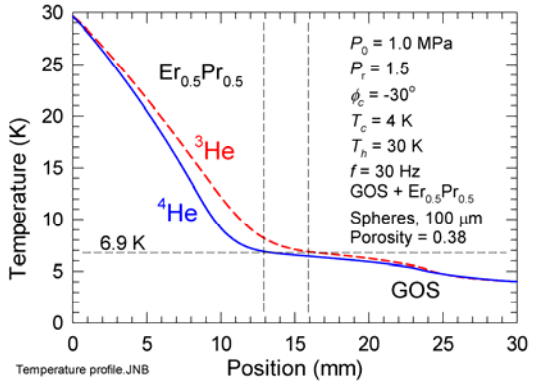

FIGURE 9. Regenerator average temperature profile showing location of layer boundary.

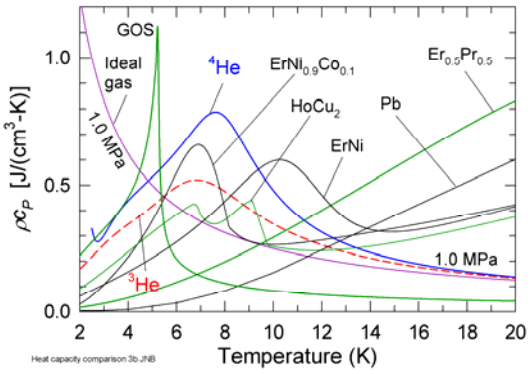

FIGURE 10. Volumetric heat capacity of several regenerator materials and helium gas.

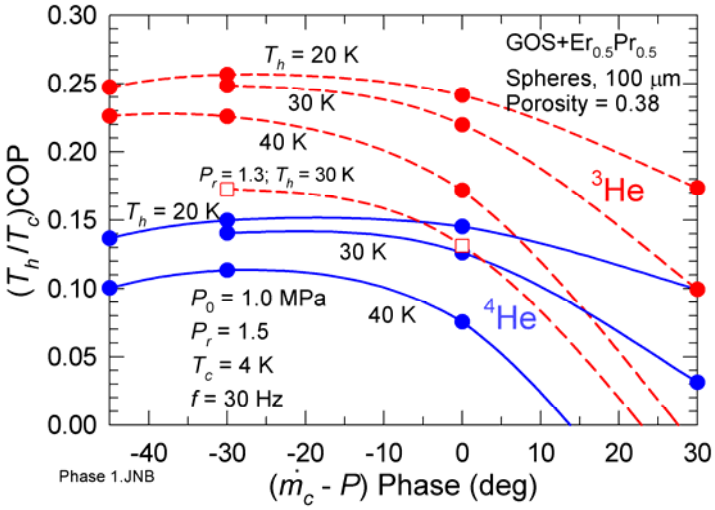

FIGURE 11. Second-law efficiency of 4 K regenerator as a function of phase ϕ_c and hot temperature.

end is at 40 K. Also shown in FIGURE 11 is the effect of pressure ratio at the cold end. If the pressure ratio is reduced from 1.5 to 1.3, the efficiency decreases significantly, and it would not be possible to achieve 4 K even with ^{3}He when the warm end is at 30 K and the phase at the cold end is +30°. This figure shows the importance of reducing ϕ_c to 0° or lower for achieving 4 K efficiently.

Effect of Flow and Hydraulic Diameter for T_h = 30 K

Most of the previous calculations were carried out by use of a flow rate that gave V_{rg}/V_E = 9.8 for ^{4}He and 7.7 for ^{3}He. As shown in FIGURE 6, such values are close to the optimum for T_h = 20 K. Because 30 K may be a better hot temperature for overall system performance, we investigated the effect of flow rate on efficiency when T_h = 30 K and ϕ_c = -30°. Both higher and lower flows led to a reduced efficiency. The results presented here have been for the case of spheres with a diameter of 100 μm and a porosity of 0.38. The sphere diameter was then varied with T_h = 30 K and ϕ_c = -30°. For 80 μm spheres the efficiency increased a negligible amount, and for 125 μm spheres the efficiency decreased 20 % for ^{4}He and 12 % for ^{3}He.

CONCLUSIONS

The NIST numerical model REGEN3.3, which incorporates the properties of both ^{4}He and ^{3}He as well as of 30 regenerator materials, was used to find the optimum set of parameters that yields the highest second-law efficiency of a 4 K regenerator operating at a frequency of 30 Hz. In all cases ^{3}He yields a higher efficiency by about a factor of two or more compared with that obtained when using ^{4}He. Because spheres of many regenerator materials are commercially available, this work focused mostly on packed spheres of 38 % porosity. A configuration using parallel holes of 25 μm diameter with a porosity of 20 % could achieve somewhat higher efficiencies, but such geometries have not been developed yet in rare-earth materials. A layered regenerator with GOS spheres at the cold end and $Er_{0.5}Pr_{0.5}$ spheres at the warm end was found to be the best material combination, although $HoCu_2$ could be substituted for GOS and achieve the same or slightly higher efficiency when the hot temperature was 30 K. Spheres of 100 μm diameter are best at the 30 Hz frequency investigated here. We found that efficiency decreased only slightly as the hot

TABLE 2. Parameter values that yield an optimized 4 K regenerator of packed spheres.

Material properties	Working fluid		^{3}He		
	Regenerator Matrix		GOS + $Er_{0.5}Pr_{0.5}$ (layered 48 %: 52 %)		
Geometry	V_{rg}/V_E	L (mm)	D_h (μm)	Config.	n_g
	5 - 8	30	41	Spheres (100 μm)	0.38
Operating conditions	P_0 (MPa)	P_r	f (Hz)	T_h (K)	ϕ_c (deg.)
	1.0	1.5	30	30	-30

temperature increased until temperatures above 35 K were used. Thus, a hot temperature of 30 K is probably best for overall system performance and simplicity for a reduced number of stages. A cold-end phase ϕ_c of -30° gives the best performance, although a phase of 0° has an efficiency only slightly lower. The efficiency for a phase of +30° is dramatically lower and will prevent reaching 4 K in many cases. TABLE 2 summarizes the optimum set of parameters for a maximum efficiency in a 4 K regenerator made with spheres. The table is for ^{3}He, but the only difference when ^{4}He is used is that the volume ratio V_{rg}/V_E should be between 7 and 10 and the layering of the regenerator matrix should be 43 % $Er_{0.5}Pr_{0.5}$ and 57 % GOS. With the conditions listed in TABLE 2 for ^{3}He, the reduced regenerator loss is 0.36 and the second law efficiency (T_h/T_c)COP is 25 %. For ^{4}He the loss is 0.51 and the efficiency is 14 %, but if $HoCu_2$ is added as an intermediate layer, the loss becomes 0.42 and the efficiency becomes 15 %. FIGURE 12 summarizes the relative entropy generation due to losses and net refrigeration for the optimized 4 K regenerator and pulse tube with both ^{4}He and ^{3}He working gas compared to an optimized regenerator and pulse tube operating at 80 K with ^{4}He. In both cases the pulse tube efficiency was taken as 80 %. This figure shows the very large real gas effects in a 4 K regenerator, especially one with ^{4}He working fluid. The large entropy generation due to the real gas effect and that due to regenerator losses leaves little entropy flow available for any net refrigeration at 4 K. However, the significant reduction of those losses when ^{3}He is the working gas allows for a much larger net refrigeration power for the same input power.

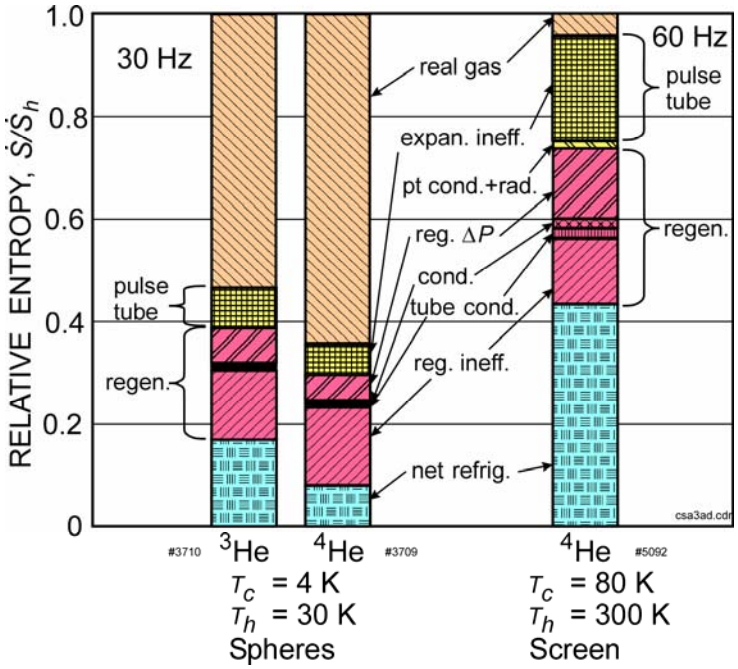

FIGURE 12. Comparison of relative entropy production due to losses and net refrigeration for an optimized 4 K regenerator/pulse tube stage with ^{3}He and ^{4}He and a 80 K regenerator/pulse tube with ^{4}He, assuming a pulse tube efficiency of 80 % and realistic conduction losses in the tube walls.

ACKNOWLEDGEMENT

This research was partially funded by the Office of Naval Research with Deborah Van Vechten as the project monitor.

REFERENCES

1. Radebaugh, R., "Refrigeration for Superconductors," in *Proc. IEEE, Special Issue on Applications of Superconductivity*, vol. 92, 2004, pp. 1719-1734.
2. Xu, M.Y., de Waele, A.T.A.M., and Ju, Y.L., "A pulse tube refrigerator below 2 K," *Cryogenics* **39**, (1999) pp. 865-869.
3. Jiang, N., Lindemann, F., Giebeler, F., and Thummes, G., "A ^{3}He pulse tube cooler operating down to 1.3 K," *Cryogenics* **44**, (2004) pp. 809-816.
4. Nast, T., Olson, J., Roth, E., Evtimov, B. Frank, D., and Champagne, P., "Development of Remote Cooling Systems for Low-Temperature, Space-Borne Systems," *Cryocoolers 14*, ICC Press, Boulder, 2007, pp. 33-40.
5. Radebaugh, R., Huang, Y., O'Gallagher, A., and Gary, J., "Calculated Regenerator Performance at 4 K: with Helium-4 and Helium-3," in *Advances in Cryogenic Engineering* 53, American Institute of Physics, 2008, pp. 225-234.
6. Radebaugh, R. , Huang, Y., O'Gallagher, A., and Gary, J., "Calculated Performance of Low-Porosity Regenerators at 4 K with He-4 and He-3," in *Cryocoolers 15*, ICC Press, Boulder, 2009, pp. 325-334.
7. Huang, Y.H., Chen, G.B., Arp, V.D., "Debye equation of state for helium-3 from 0.01 to 20 K," in *Advances in Cryogenic Engineering* 51, American Institute of Physics, 2006, pp. 879-886.
8. Huang, Y.H., Chen G.B., Arp, V., and Radebaugh, R., Equation of state and thermophysical properties of helium-3," in *Proc. International Cryogenic Engineering Conference* 21, Prague, 2006, pp. 357-362.
9. Gary, J. and Radebaugh, R., "An Improved Model for the Calculation of Regenerator Performance (REGEN3.1)," in *Proc. Fourth Interagency Meeting on Cryocoolers*, David Taylor Research Center Technical Report DTRC91/003 January 1991, pp. 165-176.
10. Numazawa, T., Yanagitani, T., Nozawa, H., Ikeya, Y., Li, R., and Satoh, T., *Cryocoolers 12*, "A New Ceramic Magnetic Regenerator material for 4 K Cryocoolers," Kluwer Academic/Plenum Press, New York, 2003, pp. 473-481.
11. Radebaugh, R., Lewis, M. Luo, E. , Pfotenhauer, J.M., Nellis, G.F., Schunk, L.A., "Inertance Tube Optimization for Pulse Tube Refrigerators," in *Advances in Cryogenic Engineering* 51, American Institute of Physics, 2006, pp. 59-67